Frustration of the isotropic-columnar phase transition of colloidal hard platelets by a transient cubatic phase: Supplementary Material

Matthieu Marechal,* Alessandro Patti,† Matthew Dennison, and Marjolein Dijkstra

Soft Condensed Matter, Debye Institute for NanoMaterials Science, Utrecht University, Princetonplein 5, 3561 RT Utrecht, The Netherlands

(Dated: February 20, 2012)

Cluster criterion

The cluster criterion consists of the following steps: First, we define the neighbors of particle i as those particles j for which the surface-to-surface distance ρ_{ij} is smaller than $0.2D$ and $\mathbf{u}_i \cdot \mathbf{u}_j > 0.9$ with $\mathbf{u}_i$ the orientation of particle i. We also define the set of particles $\mathcal{E}_i$ which contains i and its neighbors and we define the plane $\mathcal{P}_i$ perpendicular to the nematic director $\mathbf{n}_i$ of the particles in $\mathcal{E}_i$. Then, we examine the trigonal, square and hexagonal order around particle i in the plane $\mathcal{P}_i$,

$$\psi_n(i) = \left| \frac{1}{N_b(i)} \sum_{j=1}^{N_b(i)} \exp(\,\mathrm{i}\, n\phi_{ij}) \right|, \tag{1}$$

where $n = 3, 4, 6$, and ϕ_{ij} is the angle between $\mathbf{r}_{ij}^{\mathrm{proj}}$ and a reference axis, which lies in $\mathcal{P}_i$. Also, $\mathbf{r}_{ij}^{\mathrm{proj}}$ is the projection on $\mathcal{P}_i$ of the bond between particle i and j. The sum over j runs over the $N_b(i)$ neighbors of particle i which are not in the same stack as i (the values for ϕ_{ij} for j in the same stack as i are random for both isotropic and columnar phases). Furthermore, particles i and j are defined to be in the same stack if they are neighbors and their center-to-center distance r_{ij} is smaller than $L + 0.2D$. We then make a distinction between particles with a columnar-like and an isotropic-like environment. Particle i has a columnar-like environment if $\psi_6(i) > 0.6$ and $\psi_n(i) < 0.7$ for $n = 3, 4$. We define $n_{\mathrm{col}}(i)$ to be the number of particles in $\mathcal{E}_i$ that have a columnar-like environment. Those particles i that have $n_{\mathrm{col}}(i) \geq 4$ are called columnar particles. Finally, two columnar particles are part of the same cluster, if they are neighbors.

Stack rotation moves

To speed up the equilibration of Monte Carlo simulations, especially the ones with hard cut spheres and double hard cut spheres, we implemented Monte Carlo moves that are designed specifically to rotate short stacks. We select a particle randomly and define a stack by the particles with a center-to-center distance smaller than the $0.5D$. The nematic axis of this stack is determined in the usual way [1] and a random vector in the plane perpendicular to this axis is generated. The stack is rotated around this axis by ninety degrees. Finally, the move is accepted if no overlaps are generated and rejected otherwise. This move can easily be seen to obey detailed balance. Furthermore, the simulation is ergodic because regular rotation and translation moves are also performed. Although the acceptance ratio of these moves is tiny 10^{-6}, the small number of moves that are accepted during the simulation do significantly speed up the simulation.

Coexistence

We simulate two coexisting phases, a columnar phase and an isotropic or cubatic phase, in a single, rectangular simulation box. The initial configurations of these NPT MC simulations consist of two phases of interest in contact. The simulation box has to be sufficiently long in the direction perpendicular to the interface, such that the effect of the interface on either of the coexisting phases is small. While this dimension fluctuates in the simulation, the other dimensions are kept fixed at the values obtained in a prior NPT MC

* Currently at HHU, Düsseldorf, Germany
† Currently at IQAC-CSIC, Barcelona, Spain

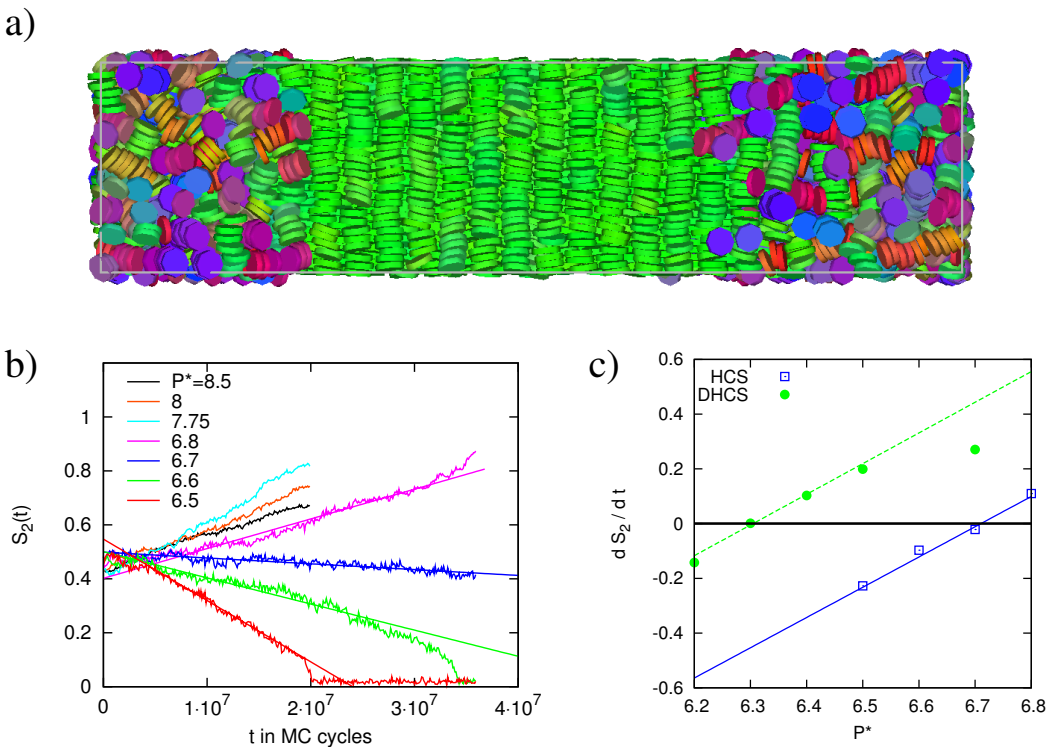

FIG. S1. (a) The initial configuration of each of the simulations in which we determine the pressure at coexistence between the isotropic phase and the columnar phase consists of a fluid phase and a columnar phase joined together in a single simulation box for cut spheres after equilibration at $P^* = 6.8$. (b) Nematic order parameter S_2 versus the number of MC cycles in NPT simulations of cut spheres at pressures $P^* \equiv \beta P v_{\rm CS}$ as labeled. The straight lines are linear fits to the straigth sections of the curves. (c) The fits from (b) as a function of the pressure P^* and the corresponding plot for double hard cut spheres. The straight lines are linear fits. The outlier for DHCS is too far from coexistence to fall on a straight line (see text) and is therefore not included in the fit.

simulation of only the bulk positionally ordered phase (the columnar phase). In the latter simulation, all three dimensions were allowed to adapt to a change in pressure. A typical snapshot of a simulation after initial equilibration, during which the cubatic phase transforms into an isotropic fluid, is shown in Fig. S1(a). In Fig. S1(b), the nematic order parameters as obtained from such simulations for cut spheres and a range of pressures are shown. Clearly the cubatic phase transforms into the columnar phase for the pressures where the fluid showed system-spanning cubatic order *i.e.* for $P^* \equiv \beta P v_{HCS} \geq 7.75$. This shows unambiguously that the cubatic phase is not stable for any of the investigated densities.

Fits to the nematic order parameter [straight lines in Fig. S1(b)] near the coexistence can be used to determine the coexistence pressure [3]. This process is shown in Fig. S1(c). The slope of the linear fits to $S_2(t)$ is denoted $d\,S_2(t)\,/\,d\,t$. The coexistence pressure is the pressure for which $d\,S_2(t)\,/\,d\,t = 0$. The growth speed can be shown to be proportional to $D[\exp(\beta\Delta\mu) - 1]$ [4], where $\Delta\mu$ is the supersaturation (the chemical-potential difference between the two phases in contact) and D is the self-diffusion constant. Near coexistence we use this to approximate $d\,S_2(t)\,/\,d\,t \simeq a\Delta\mu = a\int(1/\rho_I - 1/\rho_C)dP \simeq b\Delta P$, where ρ_I and ρ_C are the densities of the isotropic and columnar phases, respectively. Furthermore, we assume that

Shape S	$d(S,\mathrm{Cyl})$	P^*	η_I	η_C	$\eta_{\rm cub}$
DHCS	0.00165836	6.304(7)	0.4639(4)	0.5336(3)	0.495(5)
HCS	0.00653491	6.710(8)	0.4788(4)	0.5502(3)	0.505(5)
OHSC [2]	0.02527792	8.276	0.5052	0.5705	0.57(1)

TABLE I. The pressures and packing fractions at coexistence between the isotropic (I) and columnar (C) phases for HCS and DHCS from this work and for OHSC from Ref. [2]. Also shown is the Haussdorf distance $d(S,\mathrm{Cyl})$ between a cylinder (Cyl) and each of the three shapes S. Furthermore, the packing fraction $\eta_{\rm cub}$ at which the cubatic order increases suddenly on increase of the density is listed in the last column.

the pressure difference ΔP is small enough that all properties of the two phases in the simulation box are approximately equal to those of the system at coexistence, such that a and b are approximately constant. In practice, we fit a linear function to $d\,S_2(t)\,/\,d\,t$ as a function of P^* and calculate the pressure for which this straight line intersects with the line $d\,S_2(t)\,/\,d\,t = 0$ (the thick black line in Fig. S1). In Fig. S1(c), a point far from the coexistence is plotted to show that deviations from linearity are indeed a real possibility. This outlier is not included in the fit. The resulting coexistence data are listed in Tbl. I together with the data for the OHSC for reference.

Difference between shapes

The difference between shapes as plotted in the phase diagram, Fig. 5 of the main text, is defined using the Hausdorff distance [5]. In order to define this distance on shape space, which is commonly used in (convex) geometry, we first define

$$d'(A,B) = \max_{\mathbf{x}\in A}\min_{\mathbf{y}\in B}|\mathbf{x}-\mathbf{y}| \tag{2}$$

where A and B are solid (compact) bodies. The Hausdorff distance is then defined by

$$d(A,B) = \max\{d'(A,B), d'(B,A)\}. \tag{3}$$

For solid (compact) bodies, it can easily be seen that, for the two points $\mathbf{x}$ and $\mathbf{y}$ at a local minimum–maximum in Eqn. (2), (i) $\mathbf{x}$ lies on the surface ∂A of body A, while (ii) $\mathbf{y}$ lies on ∂B, (iii) $\mathbf{x}-\mathbf{y}$ is an outward normal to the surface of A in $\mathbf{x}$ and (iv) $\mathbf{x}-\mathbf{y}$ is also an outward normal to the surface of B in $\mathbf{y}$ (in the case of a cusp at one of the two points, $\mathbf{x}-\mathbf{y}$ has only to be normal to the path of the cusp at the point in question and point away from the body in question). Maximizing over all such pairs (of which there are only a few, if one takes into account the rotational symmetry) we can easily calculate the Hausdorff distance between a cylinder and an oblate hard spherocylinder, a hard cut sphere or a hard double cut sphere where all the shapes have the same aspect-ratio, volume and center-of-mass position and are co-aligned. The resulting values for the Hausdorff norm are listed in Tbl. I.

Slow and collective dynamics

In Fig. S2(a), the translational and rotational diffusion constants divided by to the respective values at $\eta = 0.5$ (near coexistence). The translational diffusion constant is defined as $\lim_{t\to\infty}\langle|\mathbf{r}_i(t)-\mathbf{r}_i(0)|^2\rangle/6t$ and the rotational diffusion constant by $\lim_{t\to\infty}\langle|\Delta\boldsymbol{\varphi}_i(t)|^2\rangle/6t$, where $\mathbf{r}_i(t)$ is the position of particle i at time t and $\Delta\boldsymbol{\varphi}_i(t)$ its angular displacement since time $t = 0$.

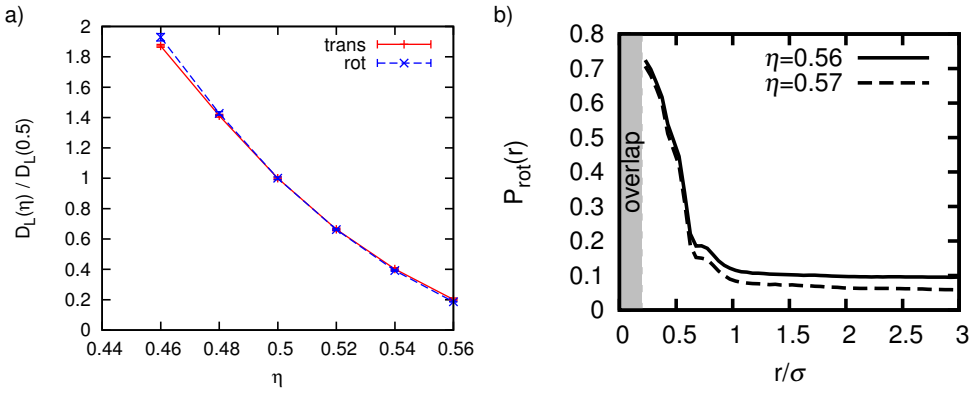

FIG. S2. (a) The rotational and translational long time diffusion constants as a function of η relative to the value at $\eta = 0.5$. For most of the density range the plots are nearl superimposed. (b) The chance $P_{\rm rot}(r) = g_{\rm rot,rot}(r)/g_{\rm rot,all}(r)$, where $g_{s,s'}(r)$ is the radial distribution function that measures the distribution of particles of type s' around particles of type s, and "all" denotes all particles, while "rot" denotes those particles that rotated more than 45 degrees between two snapshots that were taken at time intervals of $5\tau_{\rm MD}$.

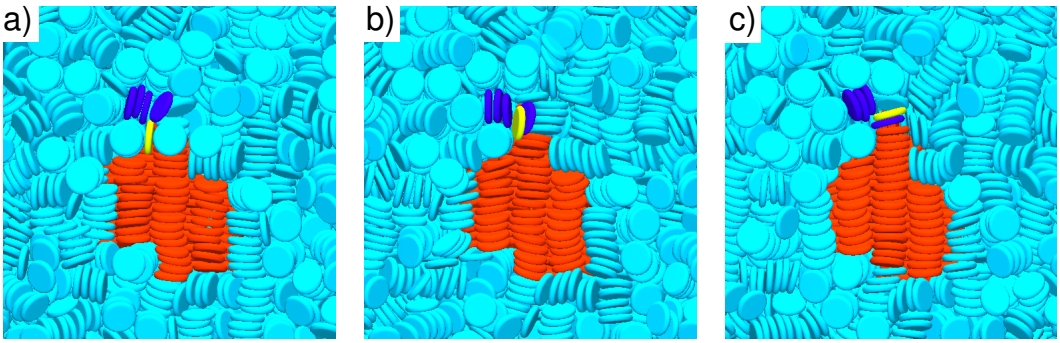

FIG. S3. (a) A particle (yellow) is misaligned with the columnar cluster (indicated by the red particles). (b) It slips in between the particles of a stack (dark blue). (c) Together with one of the particles of the stack, it rotates and becomes part of the columnar cluster.

The main mode of re-orientation is the collective rotation of the particle in a stack as can be seen in Fig. S2(c), which shows that, when a particle rotates more than 45 degrees, more than 60% of its neighbors with a center-of-mass distance smaller than $2L$ rotate along. This has consequences for the attachment to the columnar cluster, as shown in Fig. S3.

Life time of the cubatic phase

According to classical nucleation theory, the supersaturation $\Delta\mu \equiv \mu_{\rm fluid} - \mu_{\rm col}$ drives the nucleation of the columnar phase, where $\mu_{\rm fluid}$ is the chemical potential of the isotropic/cubatic branch and $\mu_{\rm col}$ the chemical potential of the columnar phase. As cubatic order is found at a much higher packing fraction for OHSC than for HSC and DHCS and the packing fraction at the IC transition only increases weakly, the supersaturation at this packing fraction $\eta_{\rm cub}$ where the cubatic order is first found is much higher for OHSC than for HCS. However, the dynamics is also much slower. Nevertheless, the cubatic phase of OHSC transforms much faster into the columnar phase for a packing fraction just above $\eta_{\rm cub}$ for OHSC, than the cubatic phase for HCS at a packing fraction even a bit higher above $\eta_{\rm cub}$ than the OHCS system, as shown in Fig. S4. For lower densities, the system of HCS never spontaneously transformed to the columnar phase in the time window accessible in our simulations.

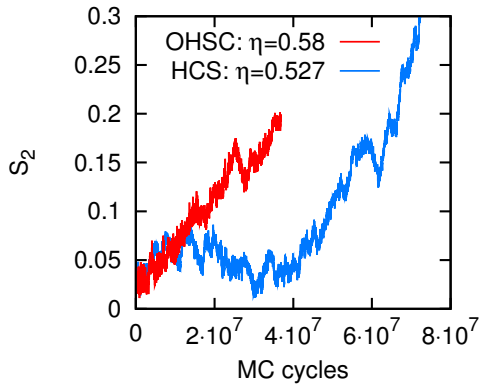

FIG. S4. The nematic order parameter S_2 for two systems as a function of the number of Monte Carlo cycles. The first system contains OHSC at $\eta = 0.58$, 2% above the isotropic–cubatic transition $\eta_{\rm cub}$, and the second HCS at $\eta = 0.58$, 4% above $\eta_{\rm cub}$.

[1] M. P. Allen, G. T. Evans, D. Frenkel, and B. M. Mulder, Advances in chemical physics **86**, 1 (1993).

[2] M. Marechal, A. Cuetos, B. Martínez-Haya, and M. Dijkstra, J. Chem. Phys. **134**, 094501 (2011).
[3] T. Zykova-Timan, J. Horbach, and K. Binder, J. Chem. Phys. **133**, 014705 (2010).
[4] S. Pronk and D. Frenkel, J. Chem. Phys. **110**, 4589 (1999).
[5] M. Moszyńska, *Selected topics in convex geometry* (Birkhäuser, Boston, 2006).